

A Novel DFIG Based Wind-Energy Conversion System with Dynamic Voltage Restorer and Energy Storage System

^{*1}K.C.Nikitha, ²Dr.V.Lakshmi Devi

^{*1}PG Scholar, Department of EEE, S.V.College of Engineering, Tirupati, Andhra Pradesh -517502

²Professor, Department of EEE, S.V.College of Engineering, Tirupati, Andhra Pradesh -517502

Corresponding Author: *nikitha.kc@gmail.com, lakshmidevi.v@svcolleges.edu.in

Abstract:

This paper proposes a novel double-fed induction generator (DFIG)-based wind-energy conversion system (WECS), which incorporates a dynamic voltage restorer (DVR) and energy storage system (ESS). The DVR is in series with the output terminal of a wind turbine generator (WTG) and parallel to the dc link of the WTG with the ESS. The control scheme of the WECS is designed to suppress wind power fluctuations and compensate grid voltage disturbances, which in turn improve the fault ride through (FRT) capability and the wind power penetration level. Finally, the performance of this WECS is investigated under various operation scenarios such as symmetrical and asymmetrical grid faults using MATLAB software.

Keywords: Wind Energy Conversion System, Dynamic Voltage Restorer, Grid Faults, Fault Ride Through Capability, Energy Storage System

Date of Submission: 02-04-2022

Date of acceptance: 16-04-2022

I. INTRODUCTION

The rapid growth of wind power has resulted in increased attention to wind-energy generation technologies [1]. Currently, there are primarily four types of wind turbine generators (WTGs), each of which has some unique characteristics [2]. The most popular WTG is the double-fed induction generator (DFIG) based WTG (DFIG-WTG), which combines the advantages conventional WTG designs and can provide approximately 40% speed variation, maximizing the amount of wind energy captured [3]. However, further development of this wind-energy generation technology is severely restricted by two important factors: wind power fluctuations, which are caused by intermittent and stochastic wind speed and can result in deviations of grid frequency and voltage, affecting the stability and power quality of grid operation [4]; the fault ride through (FRT) capability, which is required by most grid codes to tolerate voltage dips at WTG's terminal and remain connected to the grid to support voltage and frequency during and post-fault, respectively [5][6]. Several methods have been proposed to suppress wind power fluctuations. In [7] & [8], the pitch angle control is proposed to achieve flicker mitigation and stable output power level. In [9], the use of turbine inertia for power smoothing is discussed. In [10], the capability of voltage source converters to control the active power output of WTGs is also adopted to smoothen power fluctuations. However, the capability and control range of these methods are limited owing to the reduced wind power acquisition. As an alternative, energy storage systems (ESSs) have been well, indicate the increased system cost. When the dynamic voltage restorer (DVR) is introduced, a series voltage is quickly generated to correct the voltage at the WTG's terminal. Therefore, the protection control scheme inside the WTG can be greatly simplified. Here, a novel double-fed induction generator (DFIG)-based wind-energy conversion system (WECS), which incorporates a dynamic voltage restorer (DVR) and energy storage system (ESS). The performance of this WECS is investigated under various operation scenarios such as symmetrical and asymmetrical grid faults. The control scheme of the WECS is designed to suppress wind power fluctuations and compensate grid voltage disturbances, which in turn improve the fault ride through (FRT) capability and the wind power penetration level.

II. EXISTING SYSTEMS

Combining the advantages of ESS and DVR, a novel DFIG based wind-energy conversion system (WECS) is proposed, where a DVR is designed in series at the WTG's terminal and in parallel to the dc link of the WTG with the ESS. This structure is based on the modification of the system topology in [21][22] and it has the following benefits: 1) During normal operation, the ESS can absorb surplus wind power and release it when needed to smoothen the output power of the WECS. Thus, the wind power fluctuations can be greatly

suppressed and the wind power penetration level in power grid can be enhanced. 2) Under fault conditions, the DVR can quickly compensate symmetrical and asymmetrical voltage dips; hence, the voltage at the WTG's terminal is maintained and the WTG remains in operation. Further, the ESS in this case will store the blocked wind power for further potential fluctuation mitigation. A grid-side converter (GSC) is reconfigured in series between the WTG's stator and the grid during grid faults. Then, the GSC and the ESS are combined into a DVR to compensate the grid voltage disturbances. This method may reduce the cost of converters. However, it utilizes four power switches to transform operating conditions, which increases the cost and may lead to severe transients. Although the DVR and the ESS are well designed, the GSC in WECS will still suffer from grid voltage disturbances. Therefore, compared with these solutions, this novel structure could be very attractive. First, in this study, each converter inside the proposed WECS is designed for a specific control function to avoid interference and unexpected transients. Secondly, the DVR is connected at the terminal of the WTG and it can prevent the WTG from being affected by grid faults.

2.1 DOUBLY FED INDUCTION GENERATOR

A DFIG is a special type of induction generator with a wound rotor. The block diagram of the doubly fed induction generator, operating in the super synchronous mode is shown in Figure-1. The stator is directly connected to the grid. The rotor is also connected to the grid but by means of two back-to-back pulse width modulation converters. The rotor side converter is current controlled to inject the desired currents into the rotor.

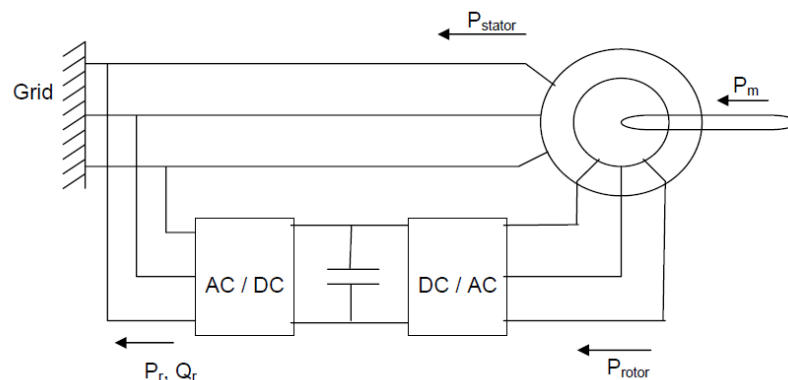


Figure-1: Structure of the doubly fed induction generator

When the machine is operating in the generating mode, the mechanical power P_m gets converted into electrical power in the stator (P_{stator}) and in the rotor (P_{rotor}). The rotor power is processed by the PWM converters and the grid side converter can be controlled to feed this power as both real and reactive powers (P_r and Q_r). Thus, the induction generator system is capable of generating a limited amount of reactive power, unlike the pitch control or rotor resistance controlled wind energy systems. The system can usually be made to operate at a unity power factor with a $\pm 10\%$ control range on the power factor for the entire system. A DFIG can operate at lagging, unity, or leading power factor and can vary its speed by a much larger margin (usually around 20 to 25 percent above or below the synchronous speed). These characteristics make the DFIG ideal for use as a wind generator. Reactive power control allows a DFIG to help provide voltage support for the grid, and variable speed operation allows the DFIG to operate at a higher efficiency over a wide range of wind speeds. The main component of the DFIG system and the conversion chain is a wind turbine, a gearbox, a DFIG and a four-quadrant power converter. The DFIG is usually designed with a low pair pole number (two or three) to obtain acceptable performance in terms of reactive power consumption. A gearbox is then necessary to adapt the low rotating speed of the wind turbine (in a range of ~ 10 -20 rpm for high-power wind turbines) to the medium-rotating speed of the DFIG. The power converter is connected between the grid and the DFIG rotor winding terminals by using slip rings. The grid side converter (GSC) is usually controlled to operate at unity power factor and to regulate the DC link voltage. The rotor side converter (RSC) controls the electrical frequency in the rotor windings and the real and reactive power flows. The rotor variable frequency supply allows the variable rotating speed operation of the wind turbine. Its rotating speed is imposed by the real power flow controlled by the RSC that is used to provide a suitable torque control loop. The reactive power managed by the RSC controls the power factor of the whole system, seen by the grid (GPF). This analysis highlights two of the DFIG's main advantages. First, a small amount of reactive power from the rotor becomes a large amount of reactive power in the stator. Second, the rotor power rating is required to be only a fraction of the entire generator rating. By proper control of the rotor converter, a DFIG's can achieve reactive power control and a wider speed range than for a cage-type induction generator. Variable speed operation allows the DFIG to

capture a greater amount of power in the wind for a given wind speed. There are three main advantages of a DFIG First, variable speed operation. Second, a small amount of rotor reactive power becomes a large amount of stator reactive power. Third, the rotor converter only needs to be rated for a fraction of the total generator rating.

III. PROPOSED SYSTEM

The proposed novel WECS is composed of three parts: the DFIG-WTG, the DVR and the ESS, as depicted in Figure2. The DVR is in series connection at the WTG's terminal. Besides, both the DVR and the ESS are connected in parallel to the dc link of the WTG.

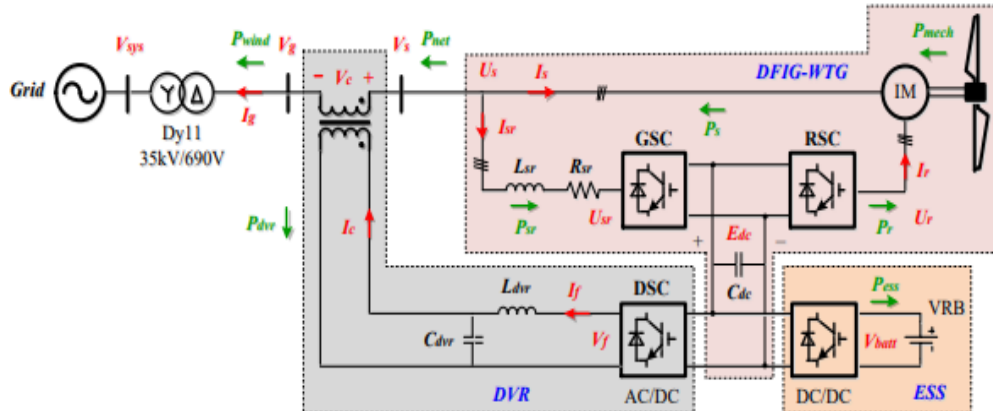


Figure-2: Structure of the novel DVR-ESS-embedded WECS

3.1 Description of DFIG-WTG:

i) *Wind turbine:* The wind turbine (WT) converts wind energy to mechanical energy by means of a torque applied to a drive train. A model of the WT is necessary to evaluate the torque and power production for a given wind speed and the effect of wind speed variations on the produced torque. The torque T and power P_m produced by the WT within the interval $[V_{min}, V_{max}]$, where V_{min} is minimum wind speed and V_{max} is maximum wind speed, are functions of the WT blade radius R , air pressure, wind speed and coefficients C_q and C_p .

$$P_m = C_p(\lambda, \beta) \frac{\rho A}{2} V_{wind}^3 \quad (1)$$

C_p is known as the power coefficient and characterizes the ability of the WT to extract energy from the wind. C_q is the torque coefficient and is related to according to:

$$C_q = \frac{C_p}{\lambda} \quad (2)$$

$$\lambda = \frac{R \cdot \omega}{V_{wind}} \quad (3)$$

$$T = \frac{P_m}{\omega} \quad (4)$$

Where,

C_p = Coefficient of performance

P_m = Mechanical output power (watt)

β = Blade pitch angle

ρ = Air density (kg/m^3)

V_{wind} = Wind speed (m/s)

A = Turbine swept area(m^2)

λ = Tip speed ratio

R = Radius of turbine blades (m)

T = Torque of wind turbine

ω = Angular frequency of rotational turbine (rad/sec).

The performance coefficient $C_p(\lambda, \beta)$, which depends on tip speed ratio λ and blade pitch angle β , determines how much of the wind kinetic energy can be captured by the wind turbine system. A nonlinear model describes $C_p(\lambda, \beta)$ as:

$$C_p(\lambda, \beta) = C_1 \left(\frac{C_2}{\lambda_1} - C_3 \beta + C_4 \right) e^{-C_5} + C_6 \quad (5)$$

Where, $C_1 = 0.5176$, $C_2 = 116$,

$C_3 = 0.4$, $C_4 = 5$, $C_5 = 21$ and

$C_6 = 0.0068$

$$\frac{1}{\lambda} = \frac{1}{\lambda + 0.08\beta} - \frac{0.035}{\beta^3 + 1} \tag{6}$$

ii) *DFIG*: Basically, the stator of the DFIG is directly linked to the grid and the rotor slip-rings are connected to the grid through the partially rated back-to-back converter. The operating principle of a DFIG can be analysed using the classic theory of rotating fields and the well-known d-q model, where the q-axis is assumed to be 90° ahead of the d-axis in the direction of rotation, and the positive current directions are defined as feeding the generator [28][30].

iii) *Rotor side converter (RSC) & Grid side converter (GSC)*: The general structure of a two-level voltage source converter (VSC) is depicted in Figure 3(a). u_{abc} is the three-phase voltage of the ac system. u_{cabc} is the three-phase ac side voltage of the VSC. i_{sabc} and i_{cabc} are the three-phase current. u_{dc} , i_d , and i_{dc} are the dc voltage, dc current, and dc side current of the VSC, respectively. c_{dc} is the dc link capacitor. To simplify the analysis, an average-value model of the VSC, as shown in Figure 3(b), is utilized for the RSC and GSC.

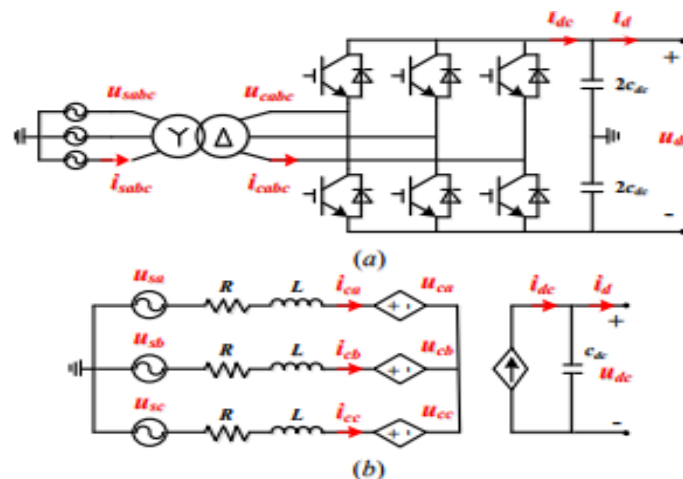


Figure-3: Structure of the two-level VSC- (a) Detailed model, (b) Average-value model.

iv) *DVR*: The DVR is a VSC connected at the WTG’s terminal and in series with the power line via three single-phase ideal transformers to correct the deteriorated grid voltages. Further, the dc side of the DVR is connected to the dc link of the WTG. Another important component of DVR is the LC filter.

v) *ESS*: A Vanadium Redox flow battery (VRB) based ESS is employed in parallel connection to the dc link of the WTG with the DVR through a DC/DC converter. The VRB is well suited for WECS applications because of its large capacity, long life, low material cost, low maintenance requirements, and fast response. The common VRB model is based on an equivalent circuit, which takes into account the physical and mathematical characteristics, as shown in Figure4.

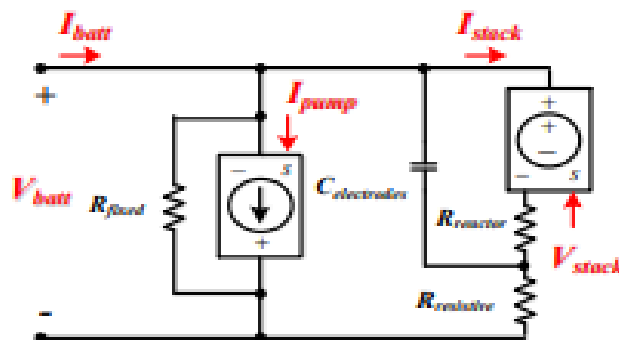


Figure-4: Equivalent circuit model of VRB

vi) *DC/DC converter*: A DC/DC converter is used to integrate the VRB-based ESS, and the circuit diagram is depicted as follows. Where Q1 and Q2 are the power switches and L_b is the inductance.

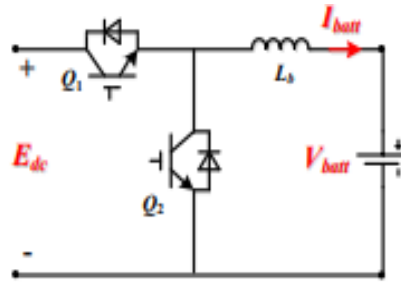


Figure-5: Bi-directional DC/DC converter

3.2 NOVEL CONTROL SCHEME FOR WECS:

From the general layout of the WECS, four power conversion systems (RSC, GSC, DSC, and DC/DC converter) are employed. Detailed control schemes for each converter are illustrated in Figure 6 below.

i) RSC: The RSC is designed to control the active and reactive power outputs of the stator P_s and Q_s. Independent control can be achieved through the rotor current control in the d-q reference frame.

ii) GSC: The function of the GSC is to control the active and reactive power outputs P_{net} and Q_{net} of the DFIG-WTG, respectively. In the same way, the independent control can be realized by the GSC current control in the d-q reference frame.

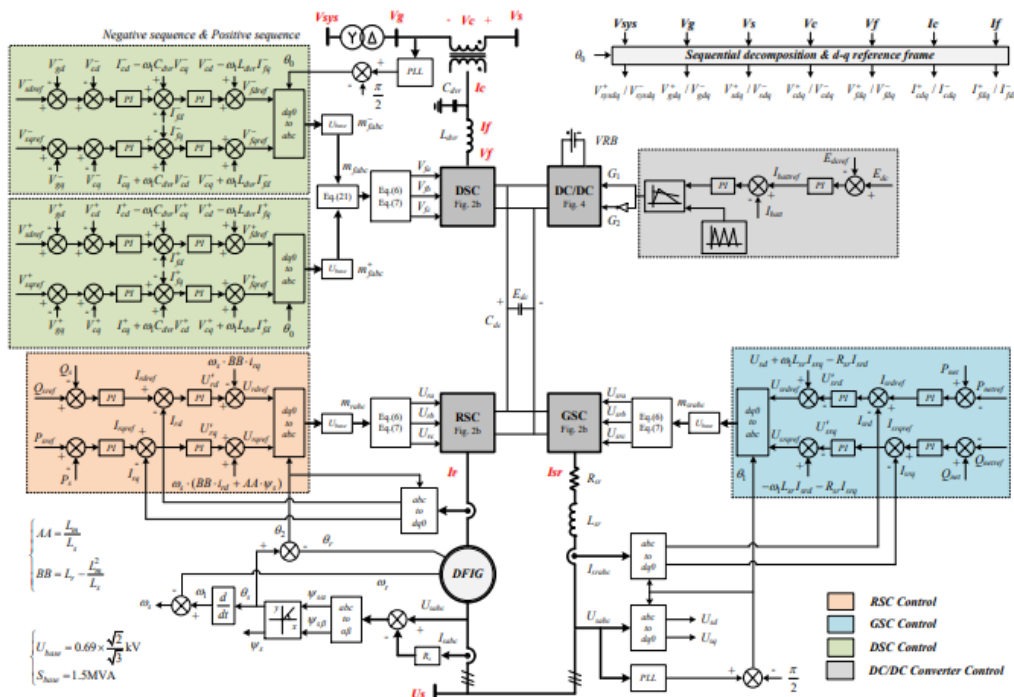


Figure-6: Control Schematic diagram of the WECS system

IV. RESULTS AND DISCUSSIONS

A 1.5MVA DFIG based WECS with embedded DVR and ESS is then modeled. The size of the VRB is 0.5MW/100kWh, and the initial SOC is 0.5. In this system, two typical scenarios are simulated to test the system performance: a) normal operation condition under time-varying wind speeds, and b) fault operation condition considering symmetrical and asymmetrical grid faults with PI controller and Genetic Algorithm methods. The results are illustrated in below figures.

Case-A: Simulation Results with PI controller strategy:

The performance of the DVR-ESS-embedded WECS under symmetrical grid fault is given in below figures. When a 0.5p.u. Balanced voltage disturbance occurs in the grid at 0.05s as shown in Figure7. The DVR can quickly generate the compensation voltage V_c in less than 0.03s as shown in Figure8 and the WTG's terminal voltage V_s can be maintained as shown in the Figure9.

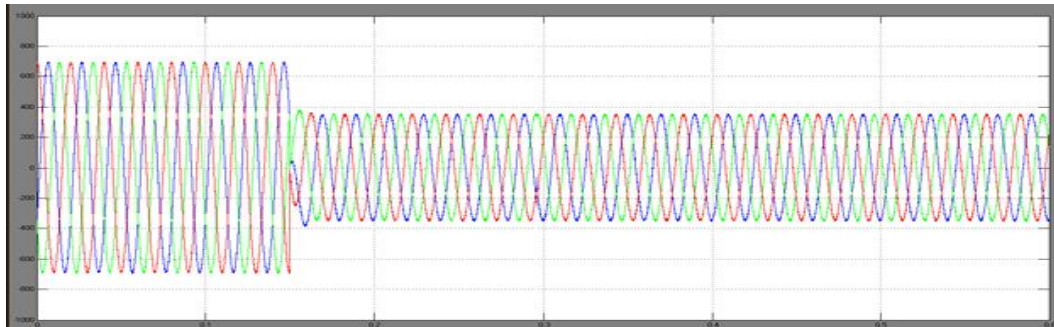


Figure-7: Disturbance in Grid voltage

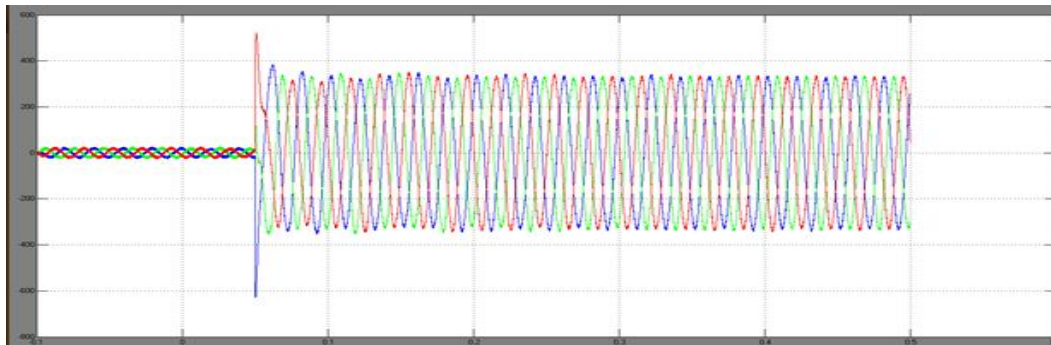


Figure-8: Compensating voltage by the DVR

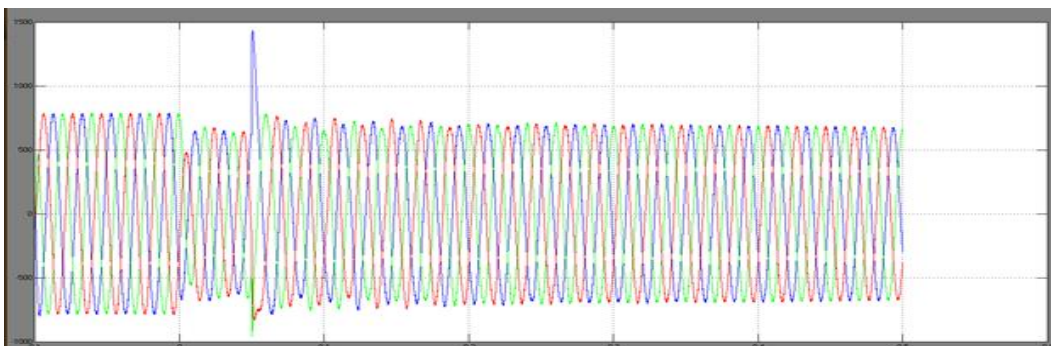


Figure-9: WTG's terminal voltage (Vs)

During the disturbance, the RMS currents of the RSC and GSC are kept below 0.5p.u. in Figure10.

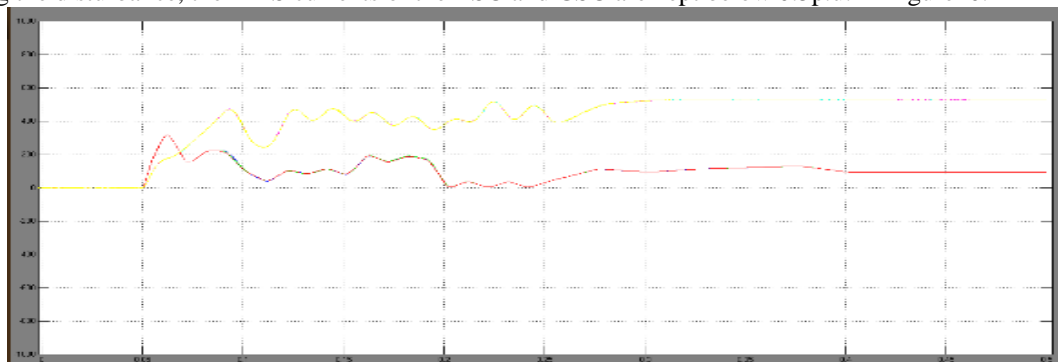


Figure-10: RMS currents of RSC and GSC

The SOC of the VRB is shown in Figure11. It decreases when the VRB discharges during the initial 0.05s, and then the SOC continues to increase.

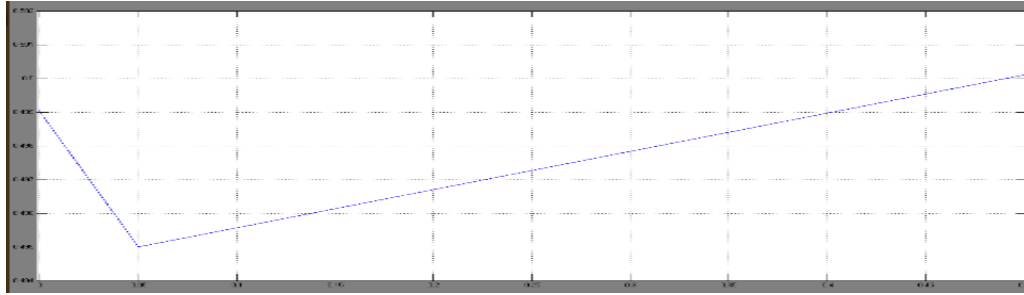


Figure-11: State of Charge of ESS (VRB)

The generated wind power P_{net} is only slightly affected, while the grid connected power P_{wind} is reduced by a half. As a result, the surplus power P_{dvr} is absorbed by the VRB as in Figure12.

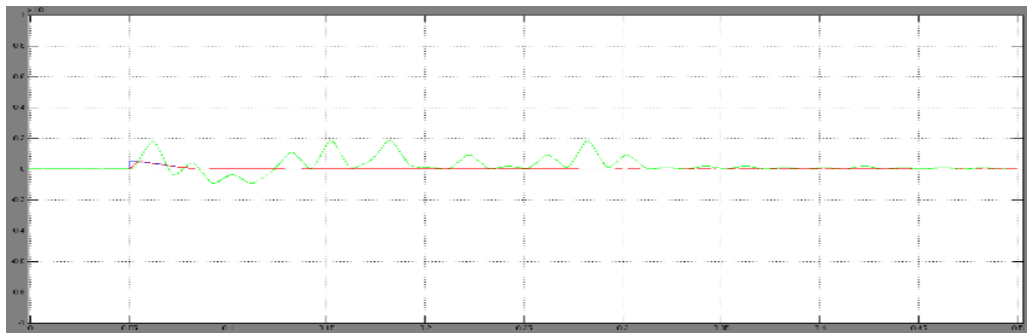


Figure-12: Power response

Besides, although a severe voltage disturbance occurs in the grid, the dc link voltage V_{dc} is slightly affected owing to the DVR compensation as shown in the Figure13.

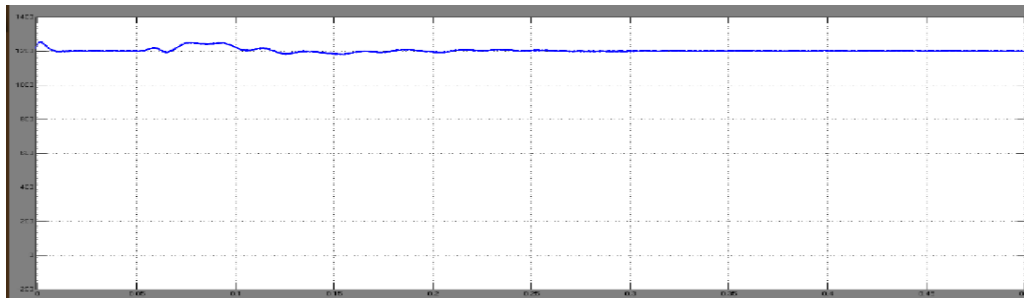


Figure-13: DC voltage

%THD of the WTG's terminal voltage (V_s) is shown in the below figure. With PI control strategy, the %THD is 5.04%.

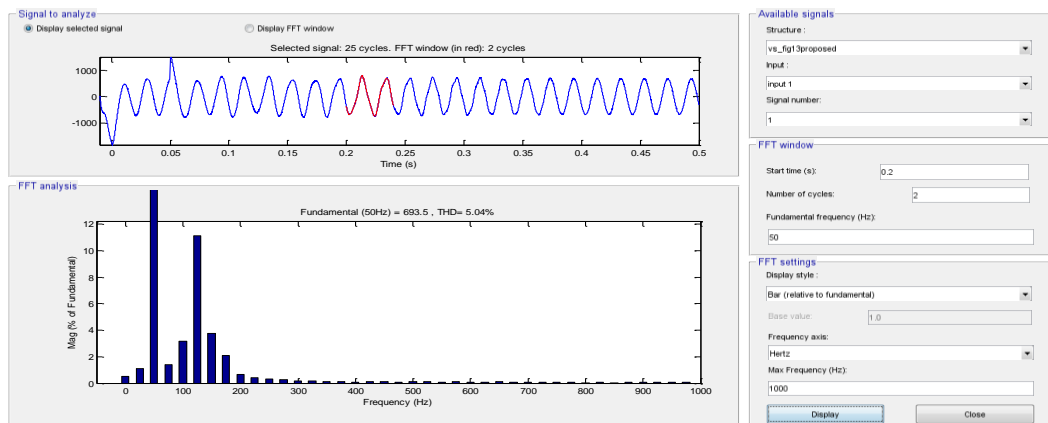


Figure-14: %THD of WTG's terminal voltage (V_s)

Case-B: Simulation results with Genetic Algorithm strategy:

The below figures shows the simulation results with Genetic Algorithm strategy applied the grid disturbances and compensation by the DVR-ESS-embedded WECS.

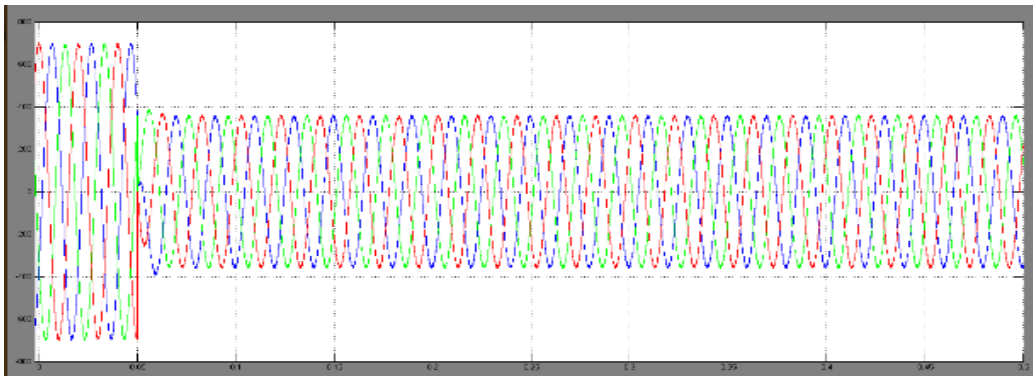


Figure-15: Disturbance in Grid voltage

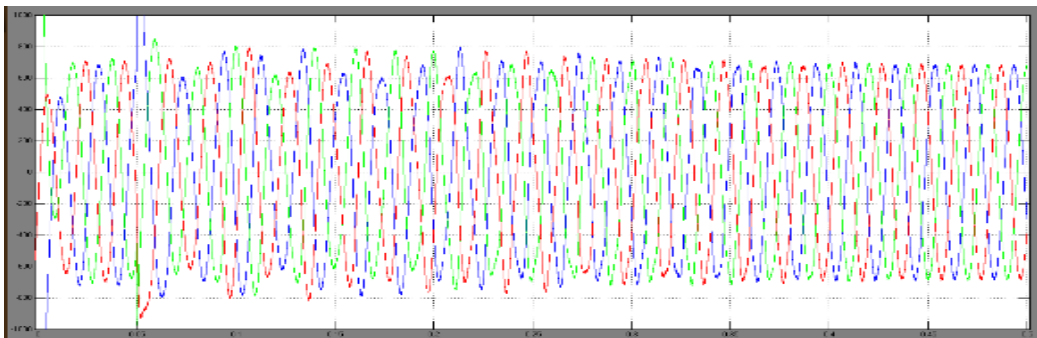


Figure-16: Compensating voltage by the DVR

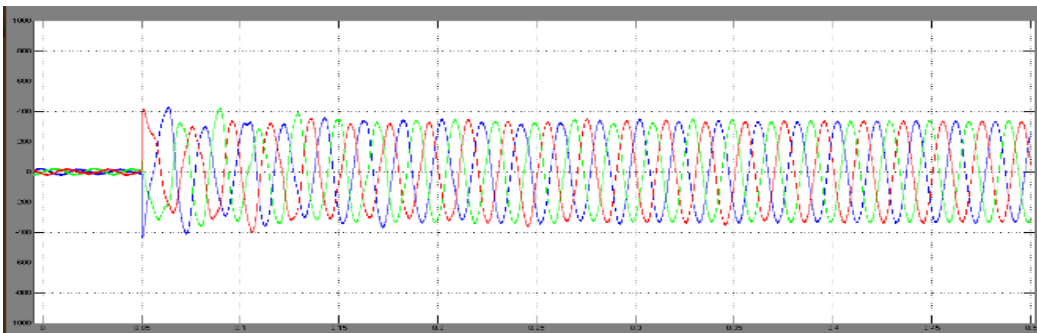


Figure-17: WTG's terminal voltage (Vs)

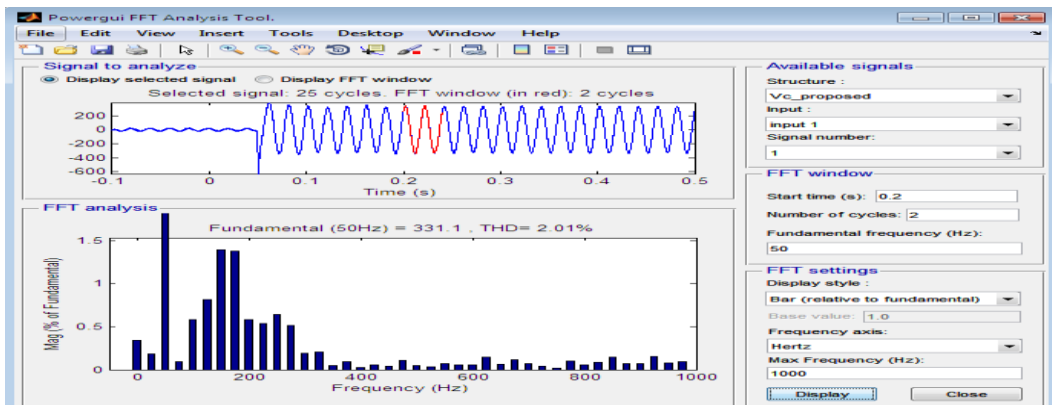


Figure-18: %THD voltage of Source Voltage

Table-1: %THD Comparison with PI Control and GA Strategies

	% OF THD OF SOURCE VOLTAGE
WITH PI CONTROLLER	5.04
WITH GENETIC ALGORITHM	2.01

V. CONCLUSIONS

In this paper, a novel DVR-ESS-embedded WECS is proposed. The system configuration and its control scheme are designed, and simulations are conducted under normal operation and fault operation conditions to test the system performance. The main conclusions are as follows. The embedded ESS can store surplus wind power for release when needed. By designing different power output commands, i.e., constant output power or filtered output power, the ESS can effectively suppress the wind power fluctuations and further improve the penetration level of wind power. The use of a DVR can significantly improve the FRT capability of the WECS under symmetrical and asymmetrical voltage fault conditions, and is particularly suitable for already installed DFIG-WTGs that do not possess sufficient FRT capability. During a disturbance, the blocked wind power generation is stored for subsequent use to suppress wind power fluctuations without any loss of energy.

REFERENCES

- [1]. T. Ackermann, "Wind Power in Power Systems," 2nd ed., Chichester: Wiley-Blackwell, 2012.
- [2]. International Electrotechnical Commission, "Grid integration of large capacity renewable energy sources and use of large capacity electrical energy storage," White paper, 2012.
- [3]. J. Yao, H. Li, Z. Chen, X. Xia, X. Chen, Q. Li, and Y. Liao, "Enhanced control of a DFIG-based wind-power generation system with series grid side converter under unbalanced grid voltage conditions," *IEEE Trans. Power Electron.*, vol. 28, no.7, pp. 3167-3181, Jul. 2013.
- [4]. S. Alaraifi, A. Moawwad, M. S. El Moursi, and V. Khadkikar, "Voltage booster schemes for fault ride-through enhancement of variable speed wind turbines," *IEEE Trans. Sustain. Energy*, vol. 4, no. 4, pp. 1071– 1081, Oct. 2013
- [5]. P. S. Flannery, and G. Venkataraman , "A fault tolerant doubly fed induction generator wind turbine using a parallel grid side rectifier and series grid side converter," *IEEE Trans. Power Electron.*, vol. 23, no. 3, pp. 1126-1135, May. 2008.
- [6]. Y. Q. Zhang, Z. Chen, W. H. Hu and M. Cheng, "Flicker mitigation by individual pitch control of variable speed wind turbines with DFIG," *IEEE Trans. Energy Convers.*, vol. 29, no. 1, pp. 20-28, Mar. 2014.
- [7]. T. Senjyu, R. Sakamoto N. Urasaki, T. Funabashi, H. Fujita and H. Sekine, "Output power leveling of wind turbine generator for all operating regions by pitch angle control," *IEEE Trans. Energy Convers.*, vol. 21, no. 2, pp. 467-475, Jun. 2006.
- [8]. E. Kamal, A. Aitouche, R. Ghorbani, and M. Bayart, "Robust fuzzy faulttolerant control of wind energy conversion systems subject to sensor faults," *IEEE Trans. Sustain. Energy*, vol. 3, no. 2, pp. 231–241, Apr. 2012. C. L. Luo, H. Banakar, B. Shen, B. Ooi, "Strategies to smooth wind power fluctuations of wind turbine generator," *IEEE Trans. Energy Convers.*, vol. 22, no. 2, pp. 341-349, Jun. 2007.
- [9]. X. Chen, L. Wang, H. Sun, and Y. Chen, "Fuzzy logic based adaptive droop control in multi-terminal HVDC for wind power integration," *IEEE Trans. Energy Convers.*, vol. 32, no. 3, pp. 1200-1208, Sept. 2017.
- [10]. J. P. Barton, D. G. Infield, "Energy Storage and Its Use with Intermittent Renewable Energy," *IEEE Trans. Energy Convers.*, vol. 19, no. 2, pp. 441-448, Jun. 2004.
- [11]. J. Q. Liang, W. Qiao and R. G. Harley, "Feed-forward transient current control for low-voltage ride-through enhancement of DFIG wind turbines," *IEEE Trans. Energy Convers.*, vol. 25, no. 3, pp. 836-843, Sept. 2010.
- [12]. L. H. Yang, Z. Xu, J. Ostgaard, Z. Y. Dong and K. P. Wang, "Advanced control strategy of DFIG wind turbines for power system fault ride through," *IEEE Trans. Power Syst.*, vol. 27, no. 2, pp. 713-722, May. 2012.
- [13]. G. Pannell, D. J. Atkinson and B. Zahawi, "Minimum-Threshold Crowbar for a Fault-Ride-Through Grid-Code-Compliant DFIG Wind Turbine," *Trans. Energy Convers.*, vol. 25, no. 3, pp. 750-759, Sept. 2010.
- [14]. J. Yang, J. E. Fletcher and J. O'Reilly, "A series-dynamic-resistor-based converter protection scheme for doubly-fed induction generator during various fault conditions," *IEEE Trans. Energy Convers.*, vol. 25, no. 2, pp. 422-432, Jun. 2010.
- [15]. X. W. Yan, G. Venkataraman , Y. Wang, Q. Dong and B. Zhang, "Grid-fault tolerant operation of a DFIG wind turbine generator using a passive resistance network," *IEEE Trans. Power Electron.*, vol. 26, no. 10, pp. 2896-2905, Oct. 2011.
- [16]. G. Pannell, B. Zahawi, D. J. Atkinson and P. Missiladis, "evaluation of the performance of a dc-link brake chopper as a DFIG low-voltage fault-ride- through device," *IEEE Trans. Energy Convers.*, vol. 28, no. 3, pp. 535-542, Sept. 2013.
- [17]. W. Qiao, G. K. Venayagamoorthy and R. G. Harley, "real-time implementation of a STATCOM on a wind farm equipped with doubly fed induction generators," *IEEE Trans. Ind. App.*, vol. 45, no. 1, pp. 98- 107, Feb. 2009.
- [18]. Y. W. Shen, D. P. Ke, W. Qiao, Y. Z. Sun, D. S. Kirschen and C. Wei, "Transient reconfiguration and coordinated control for power converters to enhance the LVRT of a DFIG wind turbine with an energy storage device," *IEEE Trans. Energy Convers.*, vol. 30, no. 4, pp. 1679-1690, Dec. 2015.
- [19]. S. Kuenzel, L. P. Kunjumammed, B. C. Pal, and I. Erlich, "Impact of wakes on wind farm inertial response," *IEEE Trans. Sustain. Energy*, vol. 5, no. 1, pp. 237–245, Jan. 2014.
- [20]. J. Lee, E. Muljadi, P. Sorensen, and Y. C. Kang, "Releasable kinetic energy-based inertial control of a DFIG wind power plant," *IEEE Trans. Sustain. Energy*, vol. 7, no. 1, pp. 279–288, Jan. 2016.